Effect Of Zinc Oxide RF Sputtering Pressure on the Structural and Optical Properties of ZnO/PEDOT:PSS Inorganic/Organic Heterojunction

Bahareh Boroomand Nasab[1], Abdolnabi Kosarian[*, 1], Navid Alaei Sheini[1]

[1] Department of Electrical Engineering, Faculty of Engineering, Shahid Chamran University of Ahvaz, Ahvaz, Iran

Abstract: Zinc oxide nanostructures are deposited on glass substrates in the presence of oxygen reactive gas at room temperature using the radio frequency magnetron sputtering technique. In this research, the effects of zinc oxide sputtering pressure on the nanostructure properties of the deposited layer are investigated. The deposition pressure varies from 7.5 to 20.5 mTorr. AFM results show that with an increase in the deposition pressure, the grain size increases and the surface roughness decreases. The energy gap measured for the zinc oxide layers deposited at the pressures of 7.5, 14 and 20.5 mTorr was 3.26, 3.18, and 3.19 eV, respectively. In order to investigate the junction between zinc oxide and poly (3, 4-ethylenedioxythiophene) polystyrene sulfonate (PEDOT:PSS), a polymeric layer of thickness of 50 nm is deposited on a 300 nm zinc oxide layer by spin coating technique. The dark I-V characteristics indicate that the reverse saturation current density is 1.82×10^{-6}, 1.96×10^{-7} and 7.58×10^{-8} A/cm^2 for the deposition pressures of 7.5, 14, and 20.5 mTorr, respectively. By increasing the deposition pressure the ideality factor of the resulting Schottky barrier dropped from 3.4 to 1.7. The effective Schottky barrier height of 0.73, 0.78, and 0.81 eV was obtained for the same order of deposition pressures. It was found that the highest optical response could be obtained for the samples deposited at the deposition pressure of 14 mTorr.

Keywords: Ideality Factor, PEDOT:PSS, Radio Frequency Magnetron Sputtering, Schottky Barrier, Zinc Oxide

1. INTRODUCTION

Zinc oxide based Schottky barrier diodes are widely used in the fabrication technology of field effect transistors [1], ultraviolet detectors [2] and gas sensors [3]. In such applications, ideality factors close to unity and Schottky barrier heights above or close to 1 eV is necessary for good device performance

---

* Corresponding author. Email: **a.kosarian@scu.ac.ir**

[4]. These parameters strongly depend on the quality of the zinc oxide layer and the interface between the zinc oxide and the Schottky contact. Several Schottky contacts (metals, oxides and polymers) have been used to enhance the device performance [5]. Schottky contacts based on PEDOT:PSS are advantageous in some aspects over the traditional Schottky contacts made of transition metals such as platinum, iridium and palladium. PEDOT:PSS is a conducting polymer with a large work function of 5.2 eV and low resistivity that can be deposited by spin coating [2].

Because of the low mobility of the carriers, the polycrystalline nature and the defect density of the interface of the zinc oxide, the performance of the devices made using thin oxide films is poor [6, 7]. Since the Schottky contact directly affects the density of the saturation current, the Schottky barrier height and the diode ideality factor, the performance of the device can be improved by proper preparation of the zinc oxide layer before deposition of the Schottky contact.

Zinc oxide, due to its physical and chemical characteristics, large energy band gap (about 3.3 eV at room temperature), high excitation binding energy (60 mV), chemical stability, transparency and electron mobility, is a good choice for optoelectronics applications. Zinc oxide is a material of group II-VI, which acts as an n-type semiconductor because of its oxygen vacancies [8].

Various growth methods have been reported for zinc oxide nanostructures, including, pulsed laser deposition [9], molecular beam deposition [10], chemical vapor deposition [11], Sol–Gel deposition [12] and sputtering [13]. Among these methods, sputtering is suitable due to the ability to deposit repeatable and homogeneous layers on a large area at low temperatures. Also, sputtering process is inexpensive compared to the most other techniques such as pulsed laser deposition and chemical vapor deposition techniques that use vacuum chamber [14, 15].

In oxide thin film based devices, the quality of the oxide layer and especially its surface properties have great impacts on the performance of the devices [16-18]. It is shown that when the ZnO nanostructures are treated with oxygen plasma after preparation, the carrier concentration and mobility of individual ZnO nanostructures decreases, while the Schottky junction behavior at the interface between the zinc oxide and the metal contact enhances with increasing the oxygen plasma treatment time [19, 20]. Annealing the ZnO layers deposited by RF magnetron sputtering in the temperature range of 250 to 450 °C indicates that post deposition annealing improves the film quality with reduced roughness and better crystalline properties [21]. The results show that surface treatments

by plasma and annealing can improve the surface properties of the zinc oxide layer, which improves its ability to measure the ultraviolet radiation.

Preparing one-dimensional compact-sized nanostructures is one of the most fundamental aspects for generating high-performance functional devices. For this purpose, this study examines the effect of deposition pressure on the quality of the zinc oxide layer and the zinc oxide/PEDOT:PSS junction.

2. EXPERIMENTAL DETAILS

For analyzing purposes, the zinc oxide nanostructures are deposited on glass substrate by radio frequency magnetron sputtering system (at 13.56 MHz) for 20 minutes. Sputtering parameters are shown in Table 1. Zinc oxide ceramic target is placed at 60 mm distance from the substrate during the sputtering process and the substrate rotates at a speed of 10 rpm for uniform deposition. In order to examine the effect of sputtering pressure on the film quality, the pressure is varied over a relatively wide range while the other parameters have been kept constant. The specimens are then analyzed using AFM, XRD and UV-VIS-NIR analysis to determine the deposition rate, surface uniformity, grain size, phase, transparency, and the energy band gap.

For device fabrication, the glass substrates coated with Indium Tin Oxide (ITO) with a sheet resistance of 8 Ω/square and thickness and 185 nm are used. Prior to the deposition at each step, the substrates were cleaned with acetone, isopropanol and deionized sonicated water and then dried with nitrogen. The sputtering coating chamber was vacuumed to a pressure less than 1×10^{-5} Torr using a diffusion pump before introducing the reactive gases. Pure oxygen and argon gases were then introduced to the chamber using appropriate flow meters. The zinc oxide layers were sputtered with the plasma power of 180 W from a zinc oxide ceramic target (99.999% purity) at 7.5, 14, and 20.5 mTorr to the thickness of 300 nm. Before the deposition, the ZnO target was pre-sputtered in argon plasma for a few minutes to clean its surface from possible contaminations. In order to form the Schottky contact, PEDOT:PSS dispersed in water was deposited on the ZnO layer using the spin coating technique. In order to protect the zinc oxide film from being etched by acidic behavior of PEDOT:PSS, it was first diluted in water (1 ml:10 ml). Afterwards, 50 µl of the diluted polymer was poured on the rotating zinc oxide layer and dried at 80° C for 20 minutes. The thickness of the deposited PEDOT:PSS layer is 50 nm. This structure was completed by using a mask to deposit 100 nm of gold by the thermal   evaporation   technique.   The   final   structure   is

Glass/ITO/ZnO/PEDOT:PSS/Au. Fig. 1 shows the mask used for the preparation of a set of three similar samples for analysis purpose. The area of each device is 0.09 cm^2.

Table 1. The sputtering parameters used for preparing the absorbing layer using a ZnO target.

Parameter	Property
Oxygen flow rate	10 sccm
Deposition Temperature	room temperature
Deposition Pressure	7.5, 14, 20.5 mTorr
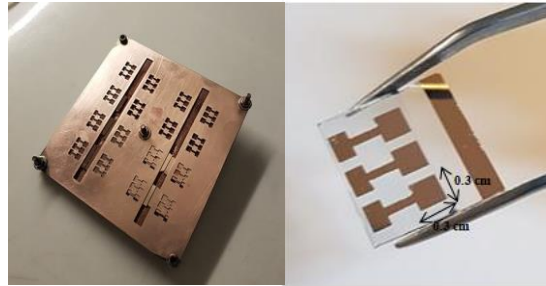
Fig. 1. The mask (left) used for preparation of three simultaneous devices (right) with similar properties.

3. RESULTS AND DISCUSSION

The microstructural properties of the specimens were investigated by the AFM analysis. As can be seen in Fig. 2, by increasing the deposition pressure from 7.5 mTorr to 20.5 mTorr the sputtering rate is gradually reduced. That is because the mean free path decreases and, as a result, the energy of the ion collisions with the substrate reduces. The morphology of the sputtered zinc oxide layers was also obtained by the AFM microscope (Fig. 3). As observed in the figure, the layers are relatively flat and uniform. Fig. 3 shows that the grain size of the layers depends heavily on the sputtering pressure. The surface roughness has been measured over an area of 2 μm × 2 μm. As observed in Fig. 3, the surface topography changes by increasing the pressure. The root mean square (RMS) of the surface roughness measured by AFM technique is 1.87, 1.14, and 0.91 nm, for the deposition pressure of 7.5, 14, and 20.5 mTorr, respectively. The AFM images show that, after 20 minutes sputtering, the

thickness of the layers is 540, 360, and 240 nm for the same order of deposition pressure.

Table 2 illustrates the average grain size of 36 ± 5 nm for the samples deposited at the pressure of 7.5 mTorr, while it increases to 50 ± 5 nm for the samples deposited at 14 mTorr. In addition, the diameter of the crystal columns formed at 20.5 mTorr is 47 ± 5 nm.
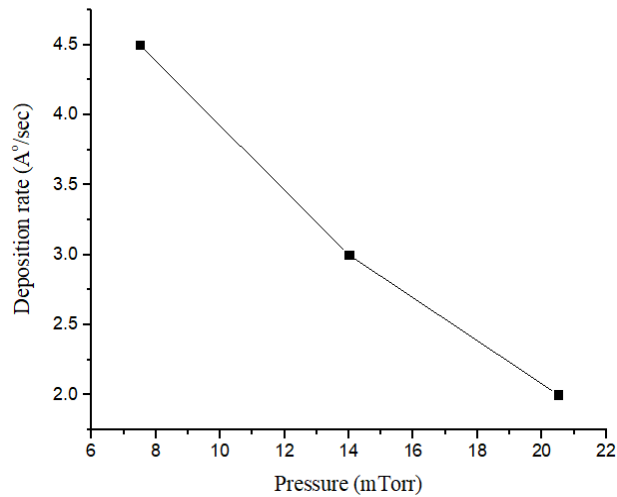
Fig. 2. Zinc oxide sputtering rate at different pressures
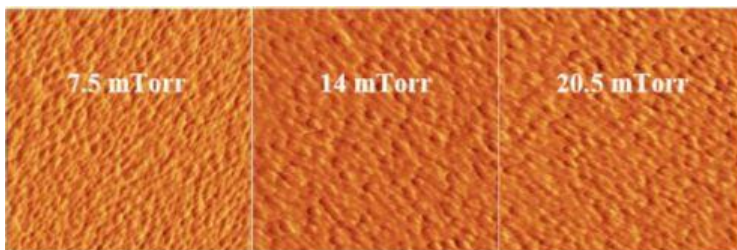
Fig. 3. Surface morphology of 2 μm × 2 μm zinc oxide layers sputtered at different pressures obtained from AFM analysis

Table 2. Structural characteristics of the zinc oxide layers sputtered at different pressures

pressure (mTorr)	average grain size (nm)	average surface roughness Ra (nm)	rms of surface roughness Rq (nm)
7.5	36 ± 5	1.49	1.87
14	50 ± 5	0.87	1.14
20.5	47 ± 5	0.71	0.91

Fig. 4 shows the XRD pattern for the zinc oxide layers sputtered at different plasma pressures. Diffraction patterns of the layers show that at either plasma pressures there are hexagonal peaks of zinc oxide (002) related to the Wurtzite structure (based on JCPDS Card No. 36-1451). The six main peak values of (100), (002), (101), (102), (110) and (103) are seen in the high pressure sample, while the sample sputtered at 7.5 mTorr has only grown in the (002) direction. The peak intensity in the (002) direction increases significantly with increasing pressure. The peak position for the 7.5 mTorr sample is at $33.33°$ which moves to $34.41°$ with increasing the pressure to 20.5 mTorr. Non-stressed zinc oxide powder peak position (002) is at $2\theta = 34.42°$, which means that the compression stress is reduced with increasing the plasma pressure.
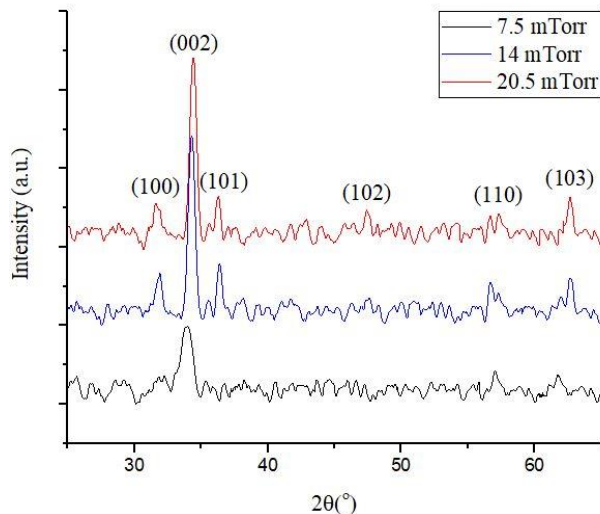
Fig. 4. X-ray diffraction pattern of the sputtered ZnO layers at different pressures

The transmittance spectra of zinc oxide layers sputtered at various pressures are shown in Fig. 5. The average transmittance of all zinc oxide layers in the visible region is more than 80%. The optical energy band gap (E_g) of the layers was estimated using the Tauc plot by extrapolating the graph of $(\alpha h\nu)^2$ versus hν. As shown in Fig. 6, the energy band gap measured for zinc oxide layers is 3.36, 3.18, and 3.19 eV at the pressures of 7.5, 14, and 20.5 mTorr, respectively.
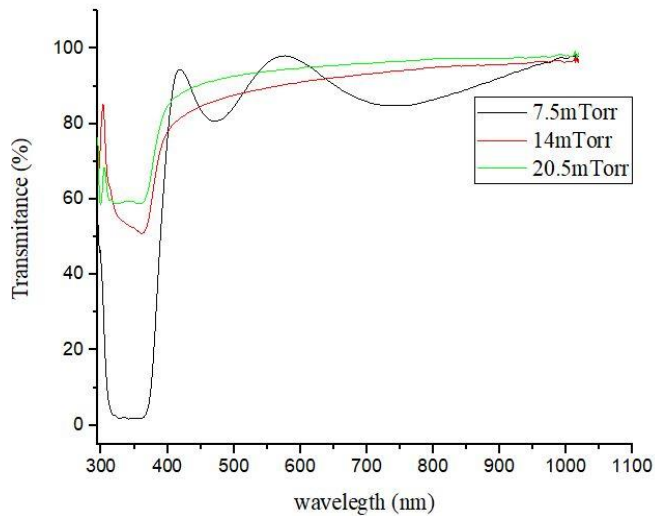
Fig. 5. The transmittance spectra of sputtered ZnO layers at different pressures

The dark current density-voltage characteristics for the glass/ITO/ZnO/PEDOT:PSS/Au structure are shown in Fig. 7. The structure is biased so that the positive and negative voltages are applied to the gold and the tin oxide layers, respectively. Each curve displayed in the figure is the average characteristics obtained from three devices prepared at the same conditions (Table 3). The characteristics clearly shows a rectifying behavior, which is due to the ZnO/PEDOT:PSS contact [22]. Since the work function of gold and PEDOT:PSS are 5.1 eV and 5.2 eV, respectively, an ohmic contact is formed at their interface. Similarly, the contact between ITO and ZnO is ohmic, since the electron affinity of ITO and ZnO are similar. Because of the different energy levels between zinc oxide and the PEDOT:PSS, a Schottky contact is formed at their interface.
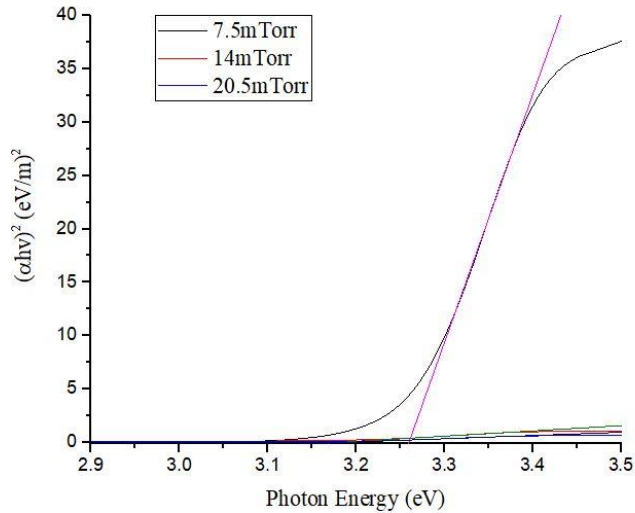
Fig. 6. The plot of (αhν)² versus photon energy (hν) for the sputtered ZnO layers at different pressures

The Schottky effect is due to the thermionic emission over the potential barrier; and the current-voltage characteristic can be described by the standard thermionic emission model. The current density relation is obtained from equation (1) [23]

$$J = J_0 \left[\exp\left(\frac{qV}{nkT} \right) - 1 \right], \tag{1}$$

where J_0 is defined as

$$J_0 = A^* T^2 \exp\left(\frac{q\Phi_{SB}}{kT} \right). \tag{2}$$

In this equation, A* is the Richardson's constant, which is estimated to be 36 A/cm2/K2 for the ZnO contact, T is the absolute temperature in kelvin, k is the Boltzmann's constant, V is the applied dc voltage, and n is the ideality factor of the diode[4].

The reverse saturation current density is obtained from the intercept of the linear part of the graph extrapolated to the vertical axis. Using this procedure, the reverse saturation current density of 1.82×10-6, 1.96×10-7 and 7.58×10-8 A/cm2 is obtained for the deposition pressures of 7.5, 14, and 20.5 mTorr, respectively. According to equation (1), the ideality factors are calculated and the values of 3.4, 2.3 and 1.7 were obtained by increasing the plasma pressure. The

Effective Schottky barrier height of 0.73, 0.78 and 0.81 eV was calculated from equation (2) for the samples prepared at the pressure of 7.5, 14 and 20.5 mTorr, respectively.
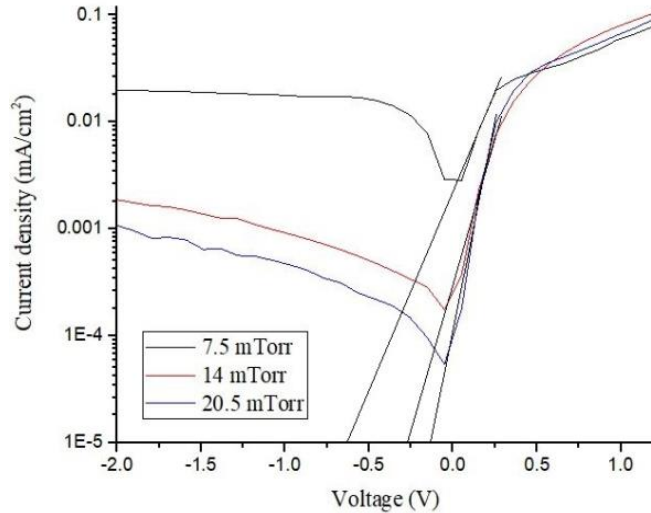
Fig. 7. Dark current density for sputtered ZnO layers at different pressures

Due to the zinc oxide optical energy band gap (around 3.2eV, which corresponds to λ=0.3875 μm), it is expected that the Schottky diode should have a good response to the ultraviolet light. The ultraviolet wavelength used in our apparatus is 365 nm. The optical response of the device to the ultraviolet light as a function of deposition pressure is shown in Fig. 8.
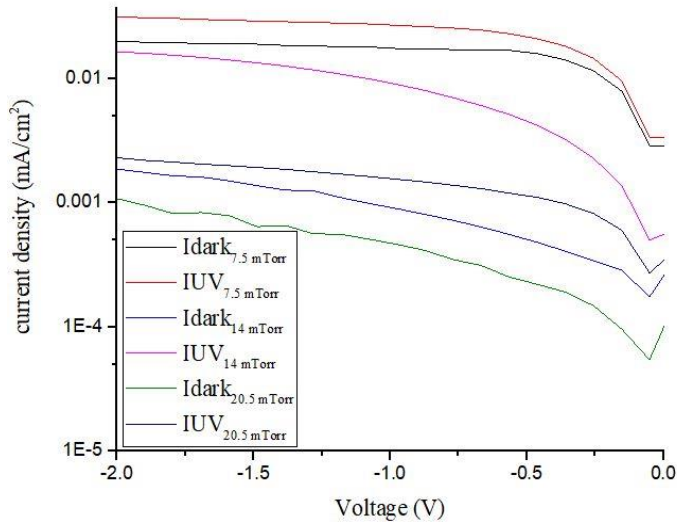
Fig. 8. Optical response for sputtered ZnO layers at different pressures

The dark current density, which is the current density under no illumination, at the reverse bias of -2 V is 1.99×10^{-5}, 1.87×10^{-6} and 1.08×10^{-6} A/cm^2 at the pressures of 7.5, 14, and 20.5 mTorr, respectively. The optical response at -2 V to the ultraviolet radiation of 8 W/cm^2 is 3.15×10^{-5}, 1.65×10^{-5} and 2.31×10^{-6} A/cm^2 for 7.5, 14, and 20.5 mTorr, respectively.

The responsivity for the device is calculated in terms of A/W using equation (3) [23]

$$R = \frac{J_{opt} - J_{dark}}{P_{opt}} \qquad (3)$$

where J_{opt} is the optical current density measured under ultraviolet radiation P_{opt} is the density of optical power illuminated on the structure. The values of responsivity R for 7.5, 14, and 20.5 mTorr are 14, 18, and 1.5 mA/W, respectively.

Table 3. Results from the analysis of Glass/ITO/ZnO/PEDOT:PSS/Au structure.

ZnO sputtering pressure (mTorr)	Saturation current density (A/cm²)	Ideality factor	Effective barrier height (eV)	Dark current density (A/cm²)	Optical current density (A/cm²)	Responsivity (mA/W)
7.5	1.82×10^{-6}	3.4	0.73	1.99×10^{-5}	3.15×10^{-5}	14
14	1.96×10^{-7}	2.3	0.78	1.87×10^{-6}	1.65×10^{-5}	18
20.5	7.58×10^{-8}	1.7	0.81	1.08×10^{-6}	2.31×10^{-6}	1.5

4. CONCLUSIONS

Zinc oxide nanostructures are successfully sputtered on glass substrates at room temperature, in the presence of oxygen reactive gas, by RF frequency magnetron sputtering system. The structural properties of nanostructures are evaluated by AFM and XRD analyzes, which show that the grain size and the magnitude of the zinc oxide main peak (002) are higher for the sample sputtered at 14 mTorr than that of the samples prepared at the pressures of 7.5 and 20.5 mTorr. The optical properties of zinc oxide nanostructures are evaluated by the UV-vis-NIR analysis, showing that the average transmittance of all layers in the visible region is higher than 80%. The results show that the optical energy band gap decreases with increasing the deposition pressure. The I-V characteristics for Glass/ITO/ZnO/PEDOT:PSS/Au structure are evaluated in the dark and under the UV radiation. The dark analysis shows that the reverse saturation current and the ideality factor will decrease with increasing the pressure, which means that the diode behavior is getting closer to the ideal by increasing the deposition pressure in the examined range. The effective Schottky barrier height for the samples prepared at the pressures of 7.5, 14, 20.5 mTorr is 0.73, 0.78, and 0.81 eV, respectively. As seen from the structural characteristics of the zinc oxide layers, an increase in the deposition pressure results in a higher crystal main peak (002) and larger grain size and at the same time the surface roughness decreases, both phenomena confirm the formation of a better junction. The optical characteristics of the devices indicate that the best response is obtained when the ZnO layer is deposited at 14 mTorr, which is due to the better absorbance behavior of the layer sputtered at this pressure compare to the layer deposited at 20.5 mTorr.

REFERENCES

[1] F. J. Klupfel, F.-L. Schein, M. Lorenz, H. Frenzel, H. von Wenckstern and M. Grundmann. *Comparison of ZnO-Based JFET, MESFET, and MISFET*. IEEE Trans. Electron Devices 60 (2013, June) 1828–1833.
Available: https://ieeexplore.ieee.org/document/6515349

[2] M. Nakano, T. Makino, A. Tsukazaki, K. Ueno, A. Ohtomo, T. Fukumura, H. Yuji, S. Akasaka, K. Tamura, K. Nakahara, T. Tanabe, A. Kamisawa, and M. Kawasaki. *Transparent polymer schottky contacts for a high performance visible-blind ultraviolet photodiode based on ZnO*. Appl. Phys. Lett. 93 (2008, Sep) 1-3.
Available: https://aip.scitation.org/doi/10.1063/1.2989125

[3] M. Shafiei, J. Yu, R. Arsat, K. Kalantar-zadeh, E. Comini, M. Ferroni, G. Sberveglieri and W. Wlodarski. *Reversed bias Pt/nanostructured ZnO Schottky diode with enhanced electric field for hydrogen sensing.* Sens. Actuators, B: Chem 146 (2010, Apr) 512-507.
Available:
https://www.sciencedirect.com/science/article/pii/S0925400509009642

[4] N. Hernandez-Como, et al. *Ultraviolet photodetectors based on low temperature processed ZnO/PEDOT:PSS Schottky barrier diode.* Materials Science in Semiconductor Processing 37 (2015, Sep) 14-18.
Available:
https://www.sciencedirect.com/science/article/pii/S1369800114007550

[5] L.J. Brillson, Y. Lu. *ZnO Schottky barriers and Ohmic contacts.* Applied Physics Letters 109 (2011, Jun) 1-33.
Available: https://aip.scitation.org/doi/10.1063/1.3581173

[6] S. Vempati, S. Chirakkara, J. Mitra, P. Dawson, K.K. Nanda and S.B. Krupanidhi. *Unusual photoresponse of indium doped ZnO/organic thin film heterojunction.* Appl. Phys. Lett 100 (2012, Mar) 1-4.
Available: https://aip.scitation.org/doi/10.1063/1.4704655

[7] D.-H. Lee, D.-H. Park, S. Kim and S. Y. Lee. *Half wave rectification of inorganic/organic heterojunction diode at the frequency of 1 kHz.* Thin Solid Films 519 (2011, Jun) 5658-5661.
Available:
https://www.sciencedirect.com/science/article/pii/S0040609011006675

[8] S. J. Mousavi. *First–Principle Calculation of the Electronic and Optical Properties of Nanolayered ZnO Polymorphs by PBE and mBJ Density Functionals.* Journal of Optoelectronical Nanostructures 2 (2017, Dec) 1-18.
Available: http://jopn.miau.ac.ir/article_2570.html

[9] S. Inguva, R. K.Vijayaraghavan, E. McGlynn and J. P. Mosnier. *High quality interconnected core/shell ZnO nanorod architectures grown by pulsed laser deposition on ZnO-seeded Si substrates.* Superlattices and Microstructures 101 (2017, Jan) 8-14.
Available:
https://www.sciencedirect.com/science/article/pii/S0749603616304669

[10] T. Yan, C.-Y. J. Lu, R. Schuber, L. Chang, D. M. Schaadt, M. M. C. Chou, K. H. Ploog and C.-M. Chiang. *Growth of c-plane ZnO on γ-LiAlO2 (1 0 0) substrate with a GaN buffer layer by plasma assisted molecular beam epitaxy.* Applied Surface Science 351 (2015, Oct) 824-830.

Available:
https://www.sciencedirect.com/science/article/pii/S0169433215013446

[11] Y. Zhao, Ch. Li, M. Chen, X. Yu, Y. Chang, A. Chen, H. Zhu and Z. Tang. *Growth of aligned ZnO nanowires via modified atmospheric pressure chemical vapor deposition*. Physics Letters A 380 (2016, Dec) 3993-3997. Available:
https://www.sciencedirect.com/science/article/abs/pii/S037596011630352 8

[12] M. Borhani Zarandi, H. Amrollahi Bioki. *Effects of Cobalt Doping on Optical Properties of ZnO Thin Films Deposited by Sol–Gel Spin Coating Technique*. Journal of Optoelectronical Nanostructures 2 (2017, Dec) 33-44.
Available: http://jopn.miau.ac.ir/article_2572.html

[13] R. Nandi and S . S. Major. *The mechanism of growth of ZnO nanorods by reactive sputtering*. Applied Surface Science 399 (2017, Dec) 305-312. Available:
https://www.sciencedirect.com/science/article/pii/S0169433216328148

[14] J. Ganji. *Concept of round non-flat thin film solar cells and their power conversion efficiency alculation*. Renewable Energy 136 (2019, Jun) 664-670.
Available:
https://www.sciencedirect.com/science/article/pii/S0960148119300333

[15] J. H. Huang, C. Y. Wang, C. P. Liu, W. H. Chu and Y.J. Chang. *Large-area growth of vertically aligned ZnO pillars by radio-frequency magnetron sputtering.* Applied Physics A 87 (2007, Jun) 749-753. Available: https://link.springer.com/article/10.1007/s00339-007-3893-0

[16] Z. Dehghani Tafti, M. Borhani Zarandi, H. Amrollahi Bioki. *Thermal Annealing Influence over Optical Properties of Thermally Evaporated SnS/CdS Bilayer Thin Films*. Journal of Optoelectronical Nanostructures 4 (2019, Mar) 87-98.
Available: http://jopn.miau.ac.ir/article_3387.html

[17] S. Manouchehri, J. Zahmatkesh, M. Hassan Yousefi. *Substrate Effects on the Structural Properties of Thin Films of Lead Sulfide*. Journal of Optoelectronical Nanostructures 3 (2018, Jun) 1-18.
Available: http://jopn.miau.ac.ir/article_2860.html

[18] M. Mahdavi Matin, M. Hakimi, M. Mazloum-Ardakani. *The effect of preparation method and presence of impurity on structural properties and*

morphology of iron oxide. Journal of Optoelectronical Nanostructures 2 (2017, Mar) 1-8.
Available: http://jopn.miau.ac.ir/article_2195.html

[19] H.-W. Ra, R. Khan, J. T. Kim, B. R. Kang, K. H. Bai and Y. H. Im. *Effects of surface modification of the individual ZnO nanowire with oxygen plasma treatment.* Materials Letters 63 (2009, Nov) 2516-2519.
Available:
https://www.sciencedirect.com/science/article/abs/pii/S0167577X0900661
2

[20] B. Angadi, H. C. Park, H. W. Choi, J. W. Choi and W. K. Choi. *Oxygen plasma treated epitaxial ZnO thin films for Schottky ultraviolet detection*. Journal of Physics D: Applied Physics 40 (2007, Feb) 1422-1425.
Available: https://iopscience.iop.org/article/10.1088/0022-3727/40/5/016/meta

[21] J. Husna, M. Mannir Aliyu, M. Aminul Islam, P. Chelvanathan, N. Radhwa Hamzah, M. Sharafat Hossain, M. R. Karim, N. Amin. *Influence of Annealing Temperature on the Properties of ZnO Thin Films Grown by Sputtering.* Energy Procedia 25 (2012, Jun) 55-61.
Available:
https://www.sciencedirect.com/science/article/pii/S1876610212011708

[22] B. K. Sharma, N. Khare and Sh. Ahmad. *A ZnO/PEDOT:PSS based inorganic/organic heterojunction*. Solid State Communications 149 (2009, Mar) 771-774.
Available:
https://www.sciencedirect.com/science/article/pii/S0038109809001203

[23] S. M. Sze and Kwok K. Ng, *Physics of Semiconductor Devices,* 3rd ed. New York, Wiley Interscience (2007).